Electronic Supplementary Material (ESI) for Chemical Communications.

This journal is © The Royal Society of Chemistry 2023

Electronic Supplementary Information (ESI)

for

From dots to tubes – the reversed scenario as bottom-up external-catalyst-free synthesis of *N*-doped carbon nanotubes

Anna Kolanowska,[a,b,*] Dariusz Łukowiec [c], Maciej Krzywiecki[d], Joanna Bok-Badura[e] and Sławomir Boncel[a,f,*]

Silesian University of Technology, Gliwice, Poland
*E-mail: anna.kolanowska@polsl.pl, slawomir.boncel@polsl.pl

[a] *NanoCarbon Group*, Faculty of Chemistry, Department of Organic Chemistry, Bioorganic Chemistry and Biotechnology, Silesian University of Technology, Krzywoustego 4, 44-100 Gliwice, Poland.

[b] Biotechnology Centre, Silesian University of Technology, Bolesława Krzywoustego 8, 44-100 Gliwice, Poland.

[c] Materials Research Laboratory, Faculty of Mechanical Engineering, Silesian University of Technology, Konarskiego 18A, 44-100 Gliwice, Poland.

[d] Institute of Physics–CSE, Silesian University of Technology, Stanisława Konarskiego 22B, 44-100 Gliwice, Poland.

[e] Faculty of Chemistry, Department of Inorganic, Analytical Chemistry and Electrochemistry, Silesian University of Technology, Krzywoustego 6, 44-100 Gliwice, Poland.

[f] Centre for Organic and Nanohybrid Electronics (CONE), Silesian University of Technology, Konarskiego 22B, 44-100 Gliwice, Poland

Table S1 Summary of the external-catalyst-free methods of the (*N*-)CNT synthesis.

CNT product	CNT properties	Procedure/ conditions /substrates	Temperature (°C)	Time (min)	Carrier gas/dopant	Carbon source	Ref.
***N*-doped SWCNTs (3.6 at.%)**	d=1.29-1.65 nm	CVD	900	1-20	$Ar/H_2/NH_3$ 1000/100/50 sccm	CH_4, 100 sccm	1
MWCNTs	d=50-100 nm l=0.6-1.6 μm	Microwave-induced pyrolysis	500	30	N_2 100 sccm	Gumwood	2
MWCNTs	d=50.3-66.1 nm	CVD, KOH-assisted	480	40	N_2 150 sccm	C_2H_2:CO_2 (1:1) 80 sccm	3
SWCNTs	d=1-2 nm	CVD, nanosized diamond	850	30	Ar, H_2 50 sccm	Ethanol	4
MWCNTs	-	CVD, Ge NPs	750	20	Ar	C_2H_2	5
SWCNTs	d=0.6-2.5 nm	CVD, Ge nanocrystals	850-1000	20	H_2 300 sccm	CH_4 1000 sccm	6
MWCNTs	d=15-50 nm	Plasma enhanced CVD	850	3-5	N_2	CH_4	7
MWCNTs	d=20-80 nm	CVD on carbon black	800	30	Ar 120 sccm	C_2H_4 40 sccm	8
MWCNTs	d=20-90 nm	CVD on graphite	850	30	He 36 sccm	C_2H_4 4 sccm	9
SWCNTs	d=1.2-1.6 nm	CVD on carbon-implanted SiGe	850	10	Ar, H_2 300 sccm	CH_4 1000 sccm	10
SWCNTs	d=1.7nm	CVD, ZnO NPs	900	20	H_2 300 sccm	Ethanol	11
SWCNTs	d<2 nm	CVD, SiO_2 or TiO_2 NPs	900	10	H_2 800 or 200 sccm, Ar 200 sccm	CH_4 200 sccm or ethanol	12
SWCNTs	d<2 nm	CVD, Te NPs	900	10	H_2 200 sccm, Ar 800 sccm	Ethanol	13
SWCNTs	-	CVD, SiO_2	900	20	H_2 500 sccm, Ar 100 sccm	CH_4 500 sccm	14
MWCNTs	-	CVD, $CaSiO_3$-coated graphite	1200-1400	60	Ar 50 sccm	Ethanol	15
MWCNTs	d<20 nm	CVD, bamboo charcoal	1200-1500	60	Ar 50 sccm	Ethanol	16
MWCNTs	d=20 nm l=0.4-9 μm	Microwave plasma enhanced CVD, amorphous carbon coated corning glass	600	5-30	H_2 80 sccm	CH_4 10 sccm	17
SWCNTs	d<2 nm	CVD, C_{60}	950	15	Ar 1000 sccm	ethanol	18
MWCNTs	d=40-80 nm	CVD, carbon black	750-1000	30	Ar 90 sscm	C_2H_2, C_2H_4, cyclohexane, ethanol 10 sccm	19
MWCNTs	d=13-16 nm	CVD, Si NPs	850	30	H_2 2000 sccm	ethanol	20
SWCNTs	-	CVD, Si/SiO_2 wafers	900	20	H_2 500 sccm	CH_4 500 sccm	21
SWCNTs	d=0.8-1.8 nm	CVD, Al_2O_3 ceramic NPs	800-850	30	Ar/H_2 300 sccm	Ethanol 50 sccm	22
MWCNTs	d=100 nm l=10 μm	Plasma assisted CVD	1727-5727	30	Ar 5000 sccm H_2 2000 sccm	Graphite rod	23
SWCNTs	d=1.0-1.8 nm	CVD, SiO_2	850	30	Ar/H_2 70 sccm	Ethanol	24
SWCNTs	d=1.0-3.0 nm	CVD, diamond NPs and fullerenes	-	-	Ar	CH_4	25
SWCNTs	d=0.9 nm l=17-52 μm	CVD, (7,6) and (6,5) SWCNTs	900	15	H_2 300 sccm Ar 160 sccm	Ethanol or CH_4 2000 sccm	26
SWCNTs	d=0.7-1.5 nm	CVD, (F-)fullerene	900	20	H_2, Ar	Ethanol	27, 28
SWCNTs	d=0.85 nm	CVD, fullerene caps	900	20	Ar, H_2 50 sccm	Ethanol	29
MWCNTs	d=50-100 nm l=0.6-1.8 μm	Microwave pyrolysis	600-1400	30	N_2 400 sccm	Cellulose	30

d – diameter, l – length, NPs – nanoparticles

Synthesis of amino-acid-CDs

Citric acid (1.5 mmol) and amino-acid (aspartic acid Asp, cysteine Cys, glycine Gly, histidine His, lysine Lys, and phenylalanine Phe) (1.5 mmol) were dissolved in distilled water (10 mL). The solution was heated in a Teflon®-coated autoclave at 180 °C for 24 h in a laboratory dryer. The autoclave was allowed to cool down to room temperature, and the post-reaction mixture was centrifuged at 5,500 rpm for 15 min. The resulting supernatant was filtered through a 0.22 µm-syringe filter (Minisart NY hydrophilic polyamide, 25 mm), and the filtrate was lyophilized (lyophilizer Martin Christ Alpha 2-4 LSCplus) to yield from yellow to dark-yellow solids.

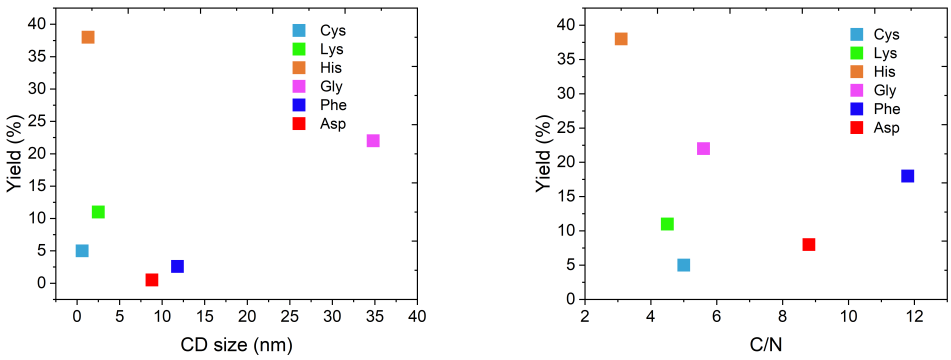

Fig. S1 The effect of: CD size (*left*), and the C/N ratio (*right*) on yield of the CD-*N*-CNT synthesis.

a)

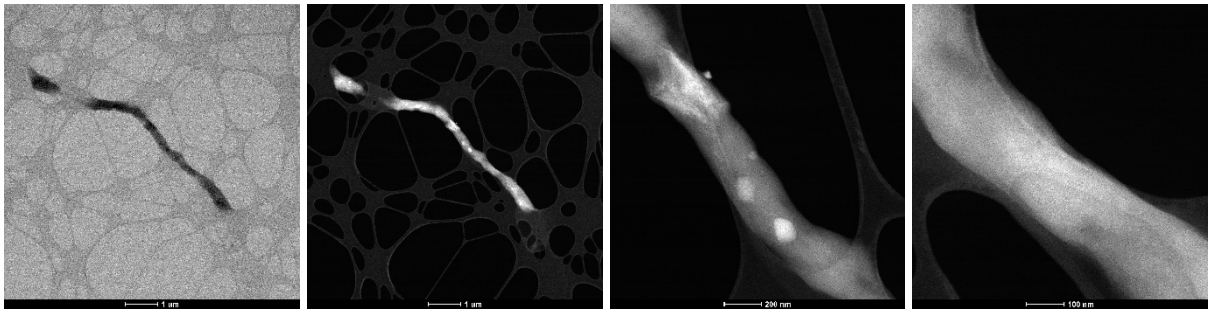

b)

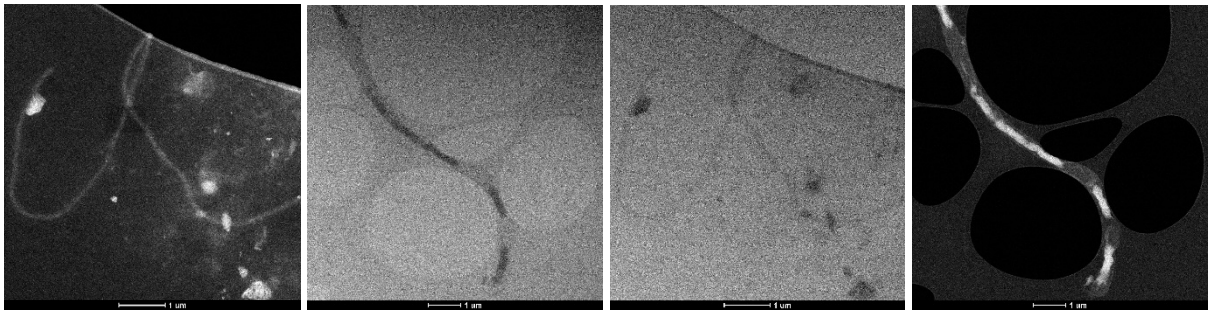

c)

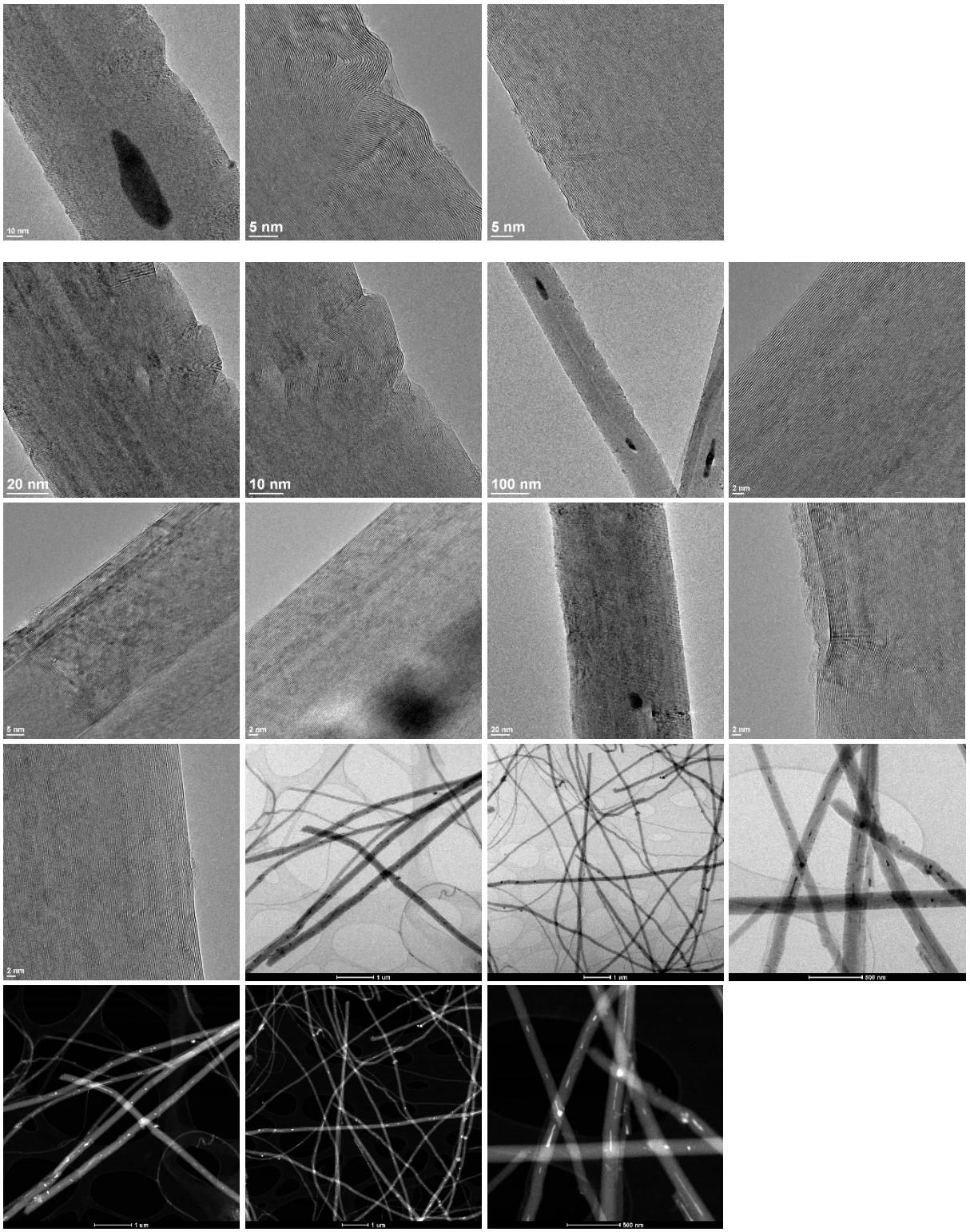

Fig. S2 A selection of bright- and dark-field TEM images of the as-synthesized: (a) His-, (b) Asp-, and (c) Phe-CD-*N*-CNTs.

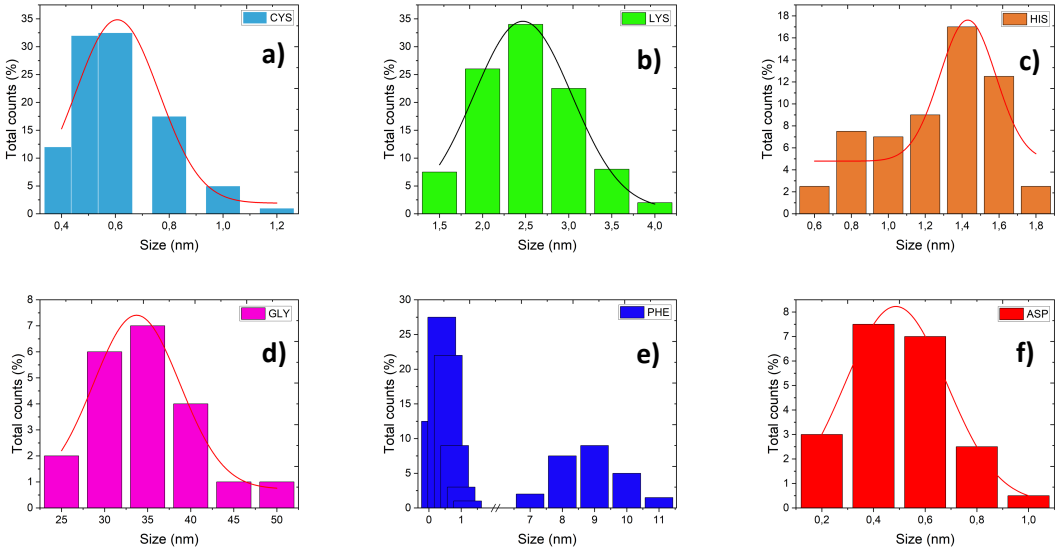

Fig. S3 DLS data of the CD volume–size distribution in the aqueous suspension under neutral pH for Cys- (a), Lys- (b), His- (c), Gly- (d), Phe- (e), and Asp-CDs (f).

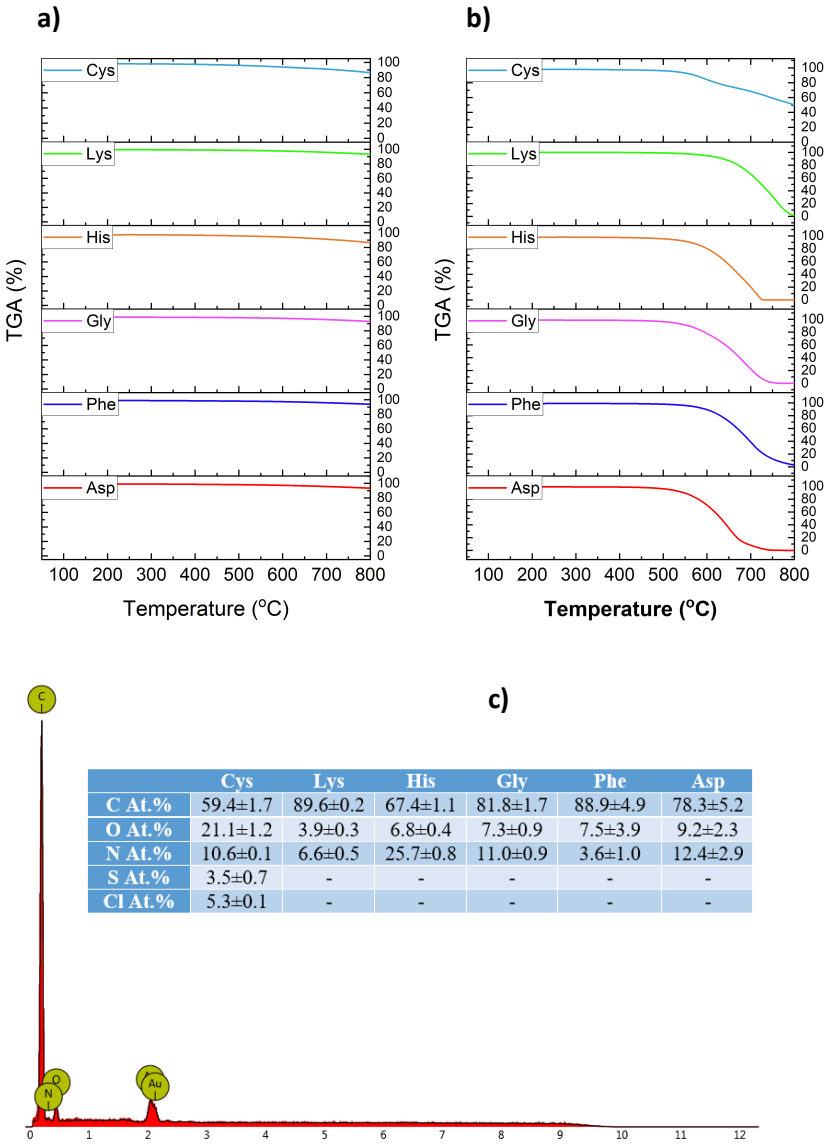

	Cys	Lys	His	Gly	Phe	Asp
C At.%	59.4±1.7	89.6±0.2	67.4±1.1	81.8±1.7	88.9±4.9	78.3±5.2
O At.%	21.1±1.2	3.9±0.3	6.8±0.4	7.3±0.9	7.5±3.9	9.2±2.3
N At.%	10.6±0.1	6.6±0.5	25.7±0.8	11.0±0.9	3.6±1.0	12.4±2.9
S At.%	3.5±0.7	-	-	-	-	-
Cl At.%	5.3±0.1	-	-	-	-	-

Fig. S4 As-synthesized amino-acid-CD-*N*-CNTs: TGA profiles under nitrogen (a) *versus* air atmosphere (b), and EDX analysis (at. %) (c).

Table S2 Raman peak intensity ratio I_D/I_G, main peak positions, and therefrom calculated L_a-values for amino acid-CD-*N*-CNTs.

	Cys-CD-*N*-CNTs	Lys-CD-*N*-CNTs	His-CD-*N*-CNTs	Gly-CD-*N*-CNTs	Phe-CD-*N*-CNTs	Asp-CD-*N*-CNTs
I_D/I_G ratio	1.14	1.12	0.99	1.03	1.07	1.10
D-band position (cm^{-1})	1346	1347	1363	1362	1346	1351
G-band position (cm^{-1})	1574	1577	1566	1588	1582	1585
L_a (nm)	34	34	39	37	36	35

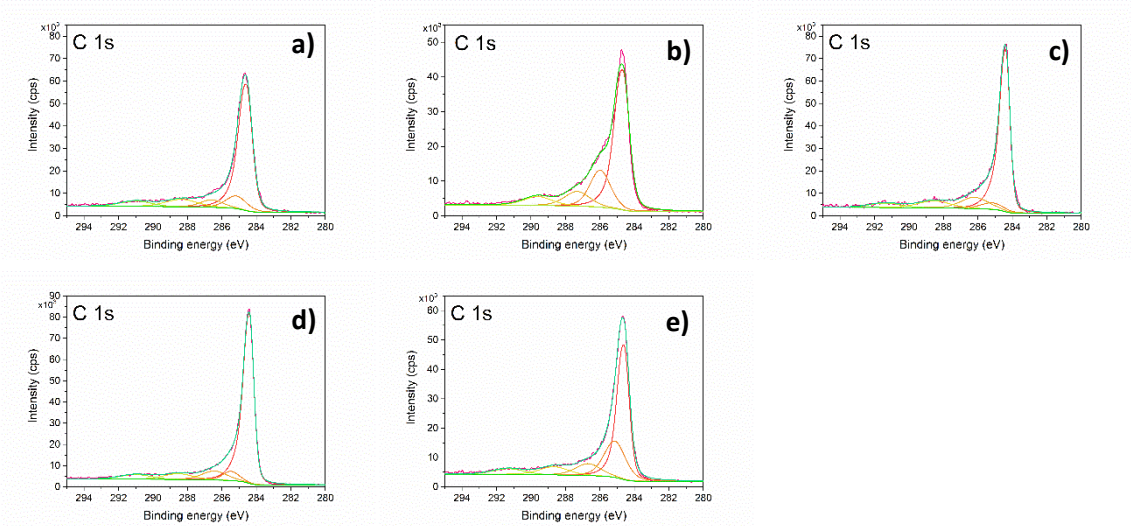

Fig. S5 XPS in the C 1s BE region for Cys- (a), Lys- (b), His- (c), Gly- (d), and Asp-CD-*N*-CNTs (e).

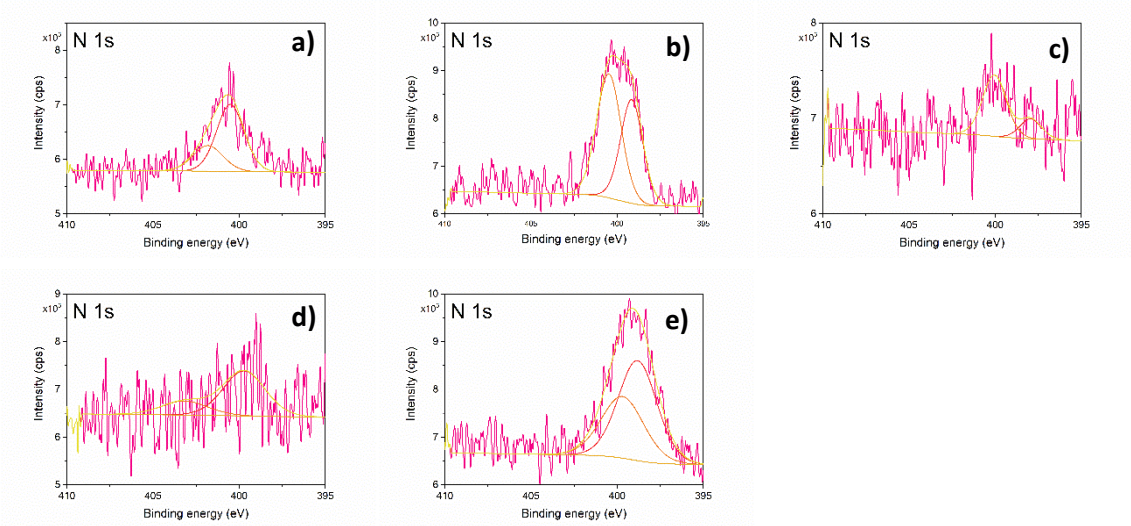

Fig. S6 XPS in the N 1s BE region for Cys- (a), Lys- (b), His- (c), Gly- (d), and Asp-CD-*N*-CNTs (e).

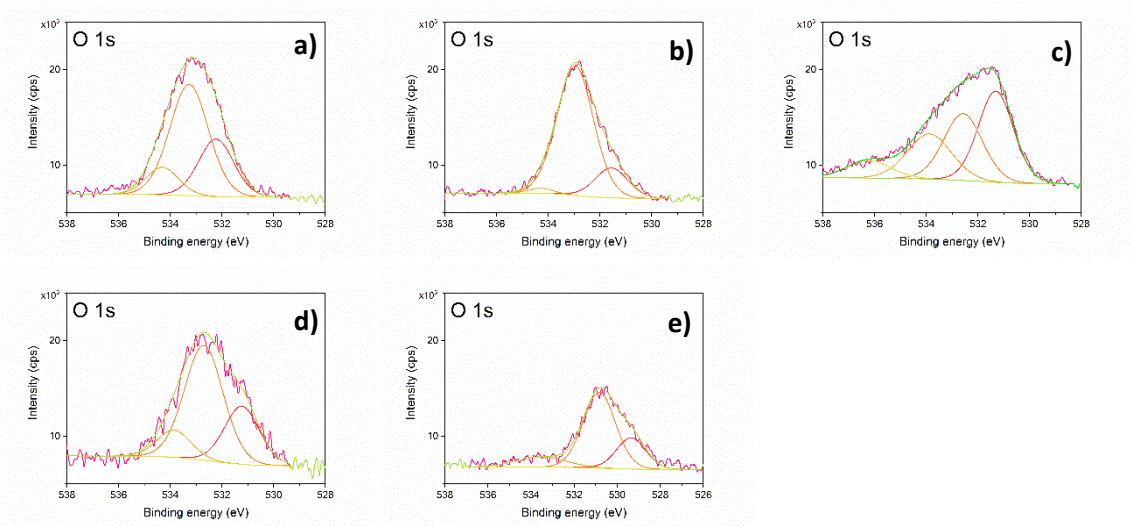

Fig. S7 XPS in the O 1s BE region for Cys- (a), Lys- (b), His- (c), Gly- (d), and Asp-CD-*N*-CNTs (e).

Table S3 Inorganic contaminants in the Phe-CD-*N*-CNTs sample determined using inductively coupled plasma atomic emission spectrometry (ICP-AES).

Sample	Al mg/l	Ca mg/l	Fe mg/l	K mg/l	Mg mg/l	Mn mg/l	Na mg/l	Pb mg/l	Zn mg/l	Co mg/l	Cu mg/l	Ni mg/l
Blank	1.06	4.25	1.14	0.66	0,60	<0.1	3.29	4.09	<0.1	<0.1	<0.1	<0.1
Phe-CD-*N*-CNTs	1.20	1.00	2.11	0.10	<0.1	<0.1	1.78	10.35	<0.1	<0.1	<0.1	<0.1
	Al mg/mg *N*-CNTs	Ca mg/mg *N*-CNTs	Fe mg/mg *N*-CNTs	K mg/mg *N*-CNTs	Mg mg/mg *N*-CNTs	Mn mg/mg *N*-CNTs	Na mg/mg *N*-CNTs	Pb mg/mg *N*-CNTs	Zn mg/mg *N*-CNTs	Co mg/mg *N*-CNTs	Cu mg/mg *N*-CNTs	Ni mg/mg *N*-CNTs
Phe-CD-*N*-CNTs	0.001197	0.001004	0.002111	9.54E-05	0.0001	0.0001	0.001785	0.01035	0.0001	0.0001	0.0001	0.0001

Preparation of the electroconductive CNT paints

Three types of CNTs: Nanocyl NC7000™, in-house synthesized ultralong MWCNTs, and Phe-CD-*N*-CNTs were dispersed in water in the presence of SDS surfactant using ultrasonication (Bandelin Sonorex RK 106, 35 kHz, 480 W) for 15 min. Next, SX-150 (screen printing base) was added. The paints were mixed for 15 min (PARKSIDE® PFBS 160 B2, 10000 rpm) and were further applied on cotton textiles at different layer thickness (50, 100, 150, 200 and 250 µm) – controlled by paint applicator Erichsen (type BIRD, model 284) – on the length of conductive path equal to 7 cm and 1.5 cm in width. Composition of the paints are listed below (Table S3). Surface electric resistances (Ω/sq) of the paths were measured using the voltage method in a custom-designed voltage measurement system.[31]

Table S4 Electroconductive CNT-based paints composition.

CNT type	CNT amount (g)	Water content (g)	SX-150 content (g)	SDS (g)	CNT content (%)	Textile weight (g)	Textile weight after coating (g)
Nanocyl NC7000 ™ MWCNTs	0.1022	1.013	0.9134	0.0010	10	0.5042	0.6247
In-house MWCNTs	0.1000	10.066	9.150	0.0010	1	0.5334	0.6048
Phe-CD-*N*-CNTs	0.1002	10.327	9.180	0.0011	1	0.4849	0.5946

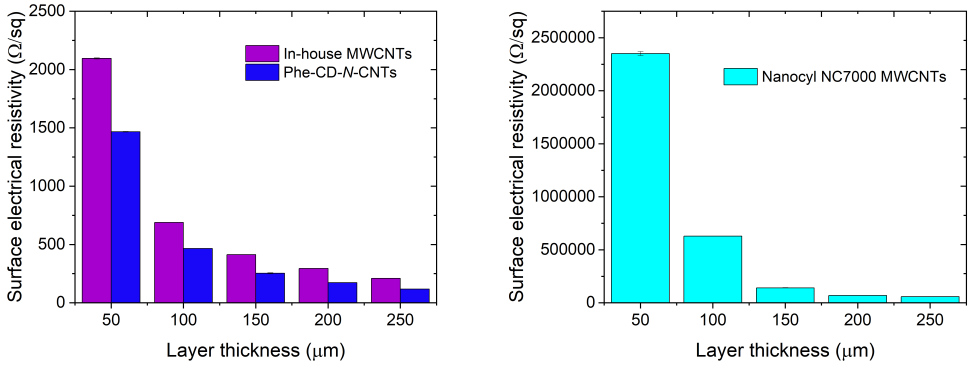

Fig. S8 Effect of coating thickness on surface electrical resistivity of Phe-CD-*N*-CNTs (navy blue), in-house MWCNTs (purple) and Nanocyl NC7000™ (turquoise) coatings on cotton.

References

1. D. Yu, Q. Zhang and L. Dai, *J Am Chem Soc Comm*, 2010, **132**, 15127-15129.
2. K. Shi, J. Yan, E. Lester and T. Wu, *Ind Eng Chem Res*, 2014, **53**, 15012-15019.
3. B.A. Tarboush, F.S. Mjalli, M.A. Alsaadi and M.M. Aljumaily, *Physica B Condens*, 2021, **621**, 413294.
4. D. Takagi, Y. Kobayashi and Y. Homma, *J Am Chem Soc*, 2009, **131**, 6922-6923.
5. A. Capasso, E. Waclawik, J.M. Bell, S. Ruffell, A. Sgarlata, M. Scarselli, M. De Crescenzi and N. Motta, *J Non Cryst Solids*, 2010, **356**, 1972-1975.
6. T. Uchino, G.N. Ayre, D.C. Smith, J.L. Hutchion, C.H. de Groot and P. Ashburn, *J Electrochem Soc*, 2009, **156**, K144-K148.
7. S. Kumar, I. Levchenko, K. Ostrikov and J.A. McLaughlin, *Carbon*, 2012, **50**, 325-329.
8. J.-H. Lin, C.-S. Chen, H.-L. Ma, C.-W. Chang, C.-Y. Hsu and H.-W. Chen, *Carbon*, 2008, **46**, 1619-1623.
9. J.H. Lin, C.S. Chen, M.H. Rummeli, A. Bachmatiuk, Z.Y. Zeng, H.L. Ma, B. Buchner and H.W. Chen, *Chem Mater*, 2011, **23**, 1637-1639.
10. T. Uchino, K.N. Bourdakos, C.H. de Groot, P. Ashburn, M.E. Kiziroglou, G.D. Dilliway and D.C. Smith, *Appl Phys Lett*, 2005, **86**, 233110.
11. F. Gao, L. Zhang and S. Huang, *Appl Surf Sci*, 2010, **256**, 2323-2326.
12. S. Huang, Q. Cai, J. Chen, Y. Qian and L. Zhang, *J Am Chem Soc*, 2009, **131**, 2094-2095.
13. Y. Qian, S. Huang, Y. Bai, J. Chen, L. Zhang, W. Guang and S. Wang, *Chem Vap Deposition*, 2010, **16**, 136-142.
14. B. Liu, W. Ren, L. Gao, S. Li, S. Pei, C. Liu, C. Jiang and H.-M. Cheng, *J Am Chem Soc*, 2009, **131**, 2082-2083.
15. J. Zhu, J. Jia, F.-L. Kwong, D.H.L. Ng and P.A. Crozier, *Carbon*, 2012, **50**, 2666-2669.
16. J. Zhu, J. Jia, F.L. Kwong, D.H.L. Ng and S.C. Tjong, *Biomass Bioenergy*, 2012, **36**, 12-19.
17. J.K. Seo, H. Jung, J.-H. Lee, S.Y. Deok, J.J. Young and W.S. Choi, *Curr Appl Phys*, 2010, **10**, S447-S450.
18. Y. Sun, R. Kitaura, J. Zhang, Y. Miyata and H. Shinohara, *Carbon*, 2014, **68**, 80-86.
19. Z.-Y. Zeng and J.-H. Lin, *RSC Adv*, 2014, **4**, 40251-40258.
20. X. Xu, S. Huang, Y. Hu, J. Lu and Z. Yang, *Mater Chem Phys*, 2012, **133**, 95-102.
21. B. Liu, D.M. Tan, C.H. Sun, C.H. Liu, C. Liu, W.C. Ren, F. Li, W.J. Yu, L.C. Yin, L.L. Zhang, C.B. Jiang and H. M. Cheng, *J Am Chem Soc*, 2011, **133**, 197-199.
22. H. Liu, D. Takagi, H. Ohno, S. Chiashi, T. Chokan and Y. Homma, *Appl Phys Express*, 2008, **1**, 014001.
23. A. Koshio, M. Yudasaka and S. Iijima, *Chem Phys Lett*, 2002, **356**, 595-600.
24. H. Liu, D. Takagi, S. Chiashi and Y. Homma, *Carbon*, 2010, **48**, 114-122.
25. F. Rao, T. Li and Y. Wang, *Carbon*, 2009, **47**, 3580-3584.
26. J. Liu, C. Wang, X. Tu, B. Liu, L. Chen, M. Zheng and C. Zhou, *Nat Commun*, 2012, **3**, 1199.
27. I. Ibrahim, Y. Zhang, A. Popov, L. Dunsch, B. Buchner, G. Cuniberti and M.H. Rummeli, *Nanoscale Res Lett*, 2013, **8**, 265.
28. I. Ibrahim, A. Bachmatiuk, M.H. Rummeli, U. Wolff, A. Popov, O. Boltalina, B. Buchner and G. Cuniberti, *Phys Status Solidi B*, 2011, **248**, 2467-2470.
29. X. Yu, J. Zhang, W. Choi, J.-Y. Choi, J.M. Kim, L. Gan and Z. Liu, *Nano Lett*, 2010, **10**, 3343-3349.
30. J.E. Omoriyekomwan, A. Tahmasebi, J. Zhang and J. Yu, *Nanomaterials*, 2022, **12**, 737.
31. A. Kolanowska, A.W. Kuziel, A.P. Herman, R.G. Jedrysiak, T. Gizewski and S. Boncel, *Prog Org Coat*, 2019, **130**, 260-269.